



Title	Bulk-Heterojunction Thin-Film Solar Cells Utilizing Miscible Binary Donor Materials of Liquid Crystalline Phthalocyanine and its Analogue
Author(s)	Fujita, Kento; Nakagawa, Dai; Nakano, Chika et al.
Citation	Journal of Physics: Conference Series. 2017, 924, p. 012003-012003
Version Type	VoR
URL	https://hdl.handle.net/11094/75680
rights	Content from this work may be used under the terms of the Creative Commons Attribution 3.0 licence. Any further distribution of this work must maintain attribution to the author(s) and the title of the work, journal citation and DOI.
Note	

The University of Osaka Institutional Knowledge Archive : OUKA

<https://ir.library.osaka-u.ac.jp/>

The University of Osaka

PAPER • OPEN ACCESS

Bulk-Heterojunction Thin-Film Solar Cells Utilizing Miscible Binary Donor Materials of Liquid Crystalline Phthalocyanine and its Analogue

To cite this article: Kento Fujita *et al* 2017 *J. Phys.: Conf. Ser.* **924** 012003

View the [article online](#) for updates and enhancements.

Related content

- [Sandwich-cell-type bulk-heterojunction organic solar cells utilizing liquid crystalline phthalocyanine](#)
Yuya Nakata, Toshiki Usui, Yuki Nishikawa *et al.*
- [Synthesis and photoelectric performance of D-A-A type small molecule based on triphenylamine](#)
Dong Yan, Yunfeng Liao, Xianwei Huang *et al.*
- [The role of multilayer graphene in the improved electrical and optical characteristics of a P3HT-based photovoltaic device](#)
Joginder Singh, Neetu Prasad, Koteswara Rao Peta *et al.*

Recent citations

- [Carrier transport and device applications of the organic semiconductor based on liquid crystalline non-peripheral octaalkyl phthalocyanine](#)
Masanori Ozaki *et al*



IOP | ebooks™

Bringing you innovative digital publishing with leading voices to create your essential collection of books in STEM research.

Start exploring the collection - download the first chapter of every title for free.

Bulk-Heterojunction Thin-Film Solar Cells Utilizing Miscible Binary Donor Materials of Liquid Crystalline Phthalocyanine and its Analogue

Kento Fujita, Dai Nakagawa, Chika Nakano, Quang-Duy Dao, Akihiko Fujii, and Masanori Ozaki

Division of Electrical, Electronic and Information Engineering, Graduate School of Engineering, Osaka University, Suita, Osaka 565-0871, Japan
E-mail: afujii@eei.eng.osaka-u.ac.jp

Abstract. Small-molecule bulk-heterojunction solar cells utilizing a binary-blended donor material composed of a liquid crystalline phthalocyanine and its analogue have been studied. The short-circuit current density (J_{sc}) and power conversion efficiency (PCE) of the solar cells utilizing the blended donor material with an optimized blend ratio reached 11.6 mA/cm² and 4.8%, respectively, which were superior to those of organic solar cells utilizing each donor material. The improvement of J_{sc} and PCE has been discussed from the viewpoints of the crystal structure, optical and carrier transport properties of the blended donor material.

1. Introduction

Recently, organic solar cells (OSC) based on solution-processed small-molecule (SM) semiconductors have attracted attention as potential alternatives to widely used conjugated polymer-based OSC [1-5]. For commercial applications, solution-processed SM semiconductors offer relatively simple synthesis and purification, monodispersity, well-defined structures without end group contaminants, relatively high charge carrier mobility, and better batch-to-batch reproducibility [3].

Some kinds of liquid crystalline (LC) materials have been demonstrated as novel SM semiconductors for organic thin-film transistors [5-7], organic light-emitting diodes [5,8,9], and solution-processed bulk-heterojunction (BHJ) OSC [9-12]. LC semiconductors exhibit the appropriate characteristics for thin-film optoelectronic devices, such as high solubility in common organic solvents and strong self-organizing nature, which lead to relatively easy fabrication of thin-films with large monodomain and high charge carrier mobility.

One of discotic LC semiconducting materials, 1,4,8,11,15,18,22,25-octahexylphthalocyanine (C6PcH₂) exhibits an ambipolar high carrier drift mobility exceeding 1 cm²/Vs in the crystalline phase, which was evaluated by time-of-flight (TOF) measurement [7]. BHJ OSC utilizing C6PcH₂ mixed with 1-(3-methoxycarbonyl)-propyl-1-phenyl-(6,6)C61 (PCBM) demonstrated high power conversion efficiency (PCE) exceeding 4% [10,13]. As further studies, fundamentals of an analogue molecule of C6PcH₂, 1,4,8,11,15,18,22,25-octahexyltetraabenzotriazaporphyrin (C6TBTAPH₂), have been reported, and high PCE exceeding 4.9% has been demonstrated in the BHJ OSC utilizing C6TBTAPH₂ mixed with 1-(3-methoxycarbonyl)propyl-1-phenyl-(6,6)C₇₁ ([70]PCBM) [14, 15].

In order to improve the photovoltaic properties of OSC with LC semiconducting materials, we focused on the miscibility. Miscibility is defined as mixing at the molecular level to produce one



homogeneous blend [16]. Introducing the concept of miscibility, improvement of the charge carrier mobility has been reported [17]. On the other hand, molecular alignment control of mixed materials has been reported [18]. Further studies have reported that the PCE of OSC was improved by utilizing the mixed donor materials, such as C6PcH₂ and its homologue molecule, 1,4,8,11,15,18,22,25-octapentylphthalocyanine (C5PcH₂) [16].

In our recent studies, it was clarified that C6TBTAPH₂ and C6PcH₂ possess the miscibility in their mixed state, that is, each molecule is mixed at the molecular level [23]. Though the PCE of BHJ OSC is expected to be improved by utilizing C6TBTAPH₂ and C6PcH₂, the detailed studies remain to be carried out.

In this study, the BHJ OSC utilizing the blended donor materials of C6TBTAPH₂ and C6PcH₂ are studied. The photovoltaic properties of the solar cells utilizing such binary donor materials are discussed by considering the absorption spectrum, crystal structure in the thin film and hole mobility in the crystal phase.

2. Experimental

C6TBTAPH₂ and C6PcH₂ were synthesized and purified as reported previously [7, 20]. [70]PCBM (Frontier carbon Ltd.) was used without further purification. The molecular structures of C6TBTAPH₂, C6PcH₂, and [70]PCBM are shown in Fig. 1.

The solar cells, the schematic device structure of which is also shown in Fig. 1, were fabricated by the following process. Indium tin oxide (ITO)-coated glass substrates were cleaned with detergent, then ultrasonicated in water, chloroform, acetone, and isopropyl alcohol, and subsequently treated with UV-induced ozone. 6-nm-thick MoO₃ film was thermally evaporated onto the ITO-coated glass substrates at a rate of 0.1 Å/s under a vacuum of about 2×10^{-5} Pa. After transferring the substrates into a N₂-filled glove box, a solution, which was prepared by dissolving the donor materials, C6TBTAPH₂ and C6PcH₂, and acceptor material, [70]PCBM in chloroform with 0.2% v/v 1,8-diiodooctane (DIO), was spin-coated onto the MoO₃ layers. The blend ratio of donor and acceptor materials and total concentration were fixed to be 13:10 mol% and 21.5 g/L, respectively. The blend ratios of C6PcH₂ in the donor materials were mainly 0, 25, 50, 75, and 100 mol%. The thickness of the active layer with the BHJ of C6TBTAPH₂:C6PcH₂: [70]PCBM, which was estimated using atomic force microscopy (AFM, Keyence VN-8000), was approximately 120 nm. Finally, 80-nm-thick aluminum electrode was deposited through a shadow mask by thermal evaporation under a vacuum of about 2×10^{-5} Pa. The active area of the device was 4 mm².

The absorption spectrum of a thin film prepared on quartz substrate was measured using a spectrophotometer (Shimadzu UV-3150) at room temperature. The energy level at the highest occupied molecular orbital (HOMO) of a material in a thin film prepared on ITO-coated glass substrate was determined by using a measurement system of photoelectron yield spectroscopy (Sumitomo Heavy Industries PYS-202-H) under a vacuum of 10^{-3} Pa at room temperature.

The current density–voltage (*J*–*V*) characteristics under an illumination from a full spectrum solar simulator (Bunkoukeiki, OTENTO-SUNIII P2) at an irradiation intensity of 100 mW/cm² (AM1.5G) were measured in vacuum at room temperature with a source measure unit (Keithley 2400). The external quantum efficiency (EQE) spectra were measured by using a photosensitivity measurement system (Bunkoukeiki, SM-250NA) with a Xe lamp light passing through a monochromator as a light source, the intensity of which was calibrated using a Si reference cell. The integrated EQE values indicated good agreements with the measured short-circuit current density (*J*_{sc}).

The charge carrier mobility under a low vacuum (10^{-1} Pa) was determined by the TOF technique. A sandwich cell consisting of two ITO-coated glass substrates and a 12-μm-thick PET spacer was fabricated. The actual cell gap was evaluated by an interference technique of light transmittance. Subsequently, binary-blended materials of C6TBTAPH₂ and C6PcH₂, which were prepared by vaporizing the solvent in the solution of C6PcH₂ and C6TBTAPH₂, were heated to a temperature in the isotropic phase for injecting into the cell by capillary action, and cooled down to room temperature

in vacuum. A DC bias was applied between the electrodes using batteries connected in series, and the films were irradiated using a Nd:YAG laser (wavelength: 355 nm, pulse width: 1 ns). The transient current response was observed using an oscilloscope (Teledyne LeCroy HDO4054) in vacuum at room temperature, and the charge carrier mobility μ was calculated according to the equation $\mu = d^2/V\tau$, where d , V , and τ are the film thickness, applied bias, and transit time, respectively.

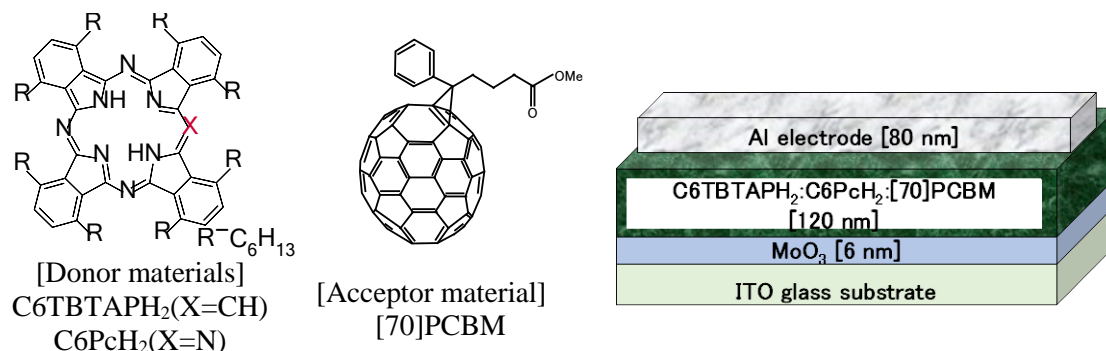


Figure 1. Molecular structures of C6TBTAPH₂, C6PcH₂, and [70]PCBM, and schematic device structure of the C6TBTAPH₂:C6PcH₂: [70]PCBM BHJ OSC.

3. Results and Discussion

Figure 2 shows the absorption spectra of C6TBTAPH₂:C6PcH₂: [70]PCBM thin films with various C6PcH₂ blend ratios. Two high absorption peaks at 300–450 nm and 600–800 nm were observed, which correspond to the optical transition at the B-band and Q-band of C6TBTAPH₂ or C6PcH₂, respectively. The absorbance of C6TBTAPH₂ at the B-band is higher than that of C6PcH₂, while the absorbance of C6TBTAPH₂ at the Q-band is lower than that of C6PcH₂ [15]. In the C6TBTAPH₂:C6PcH₂: [70]PCBM thin films, therefore, the absorbance at the B-band decreased, and that at the Q-band increased with increasing the blend ratio of C6PcH₂. It is noted that the marked change of the optical properties, such as absorption spectrum, appeared by adjusting the blend ratio of C6TBTAPH₂:C6PcH₂, in spite of the slight difference of the molecular structures.

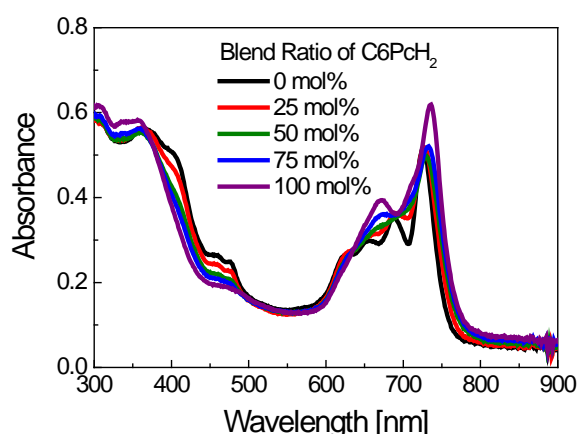


Figure 2. Absorption spectra of C6TBTAPH₂:C6PcH₂: [70]PCBM thin films with various C6PcH₂ blend ratios.

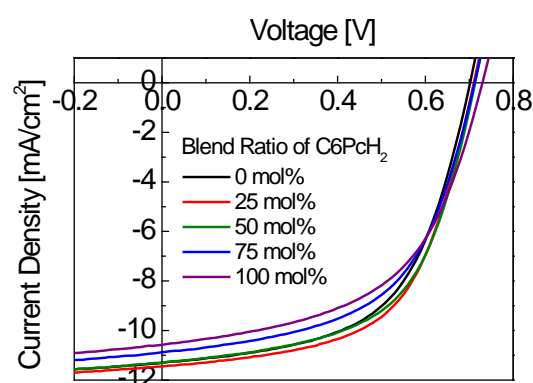


Figure 3. J - V characteristics of the C6TBTAPH₂:C6PcH₂: [70]PCBM BHJ OSC with various C6PcH₂ blend ratios.

The J - V characteristics of C6TBTAPH₂:C6PcH₂:[70]PCBM BHJ OSC are shown in Fig. 3, and the photovoltaic properties depending on the C6PcH₂ blend ratio are summarized in Table I. The open-circuit voltage (V_{oc}) of the solar cell with C6TBTAPH₂:[70]PCBM BHJ or C6PcH₂:[70]PCBM BHJ was 0.70 or 0.73 V, respectively. The V_{oc} of the solar cells with the blended donors of C6TBTAPH₂:C6PcH₂ were 0.71 V, which was close to that with C6TBTAPH₂:[70]PCBM BHJ. The V_{oc} of OSC is explained by an energy gap between the HOMO level of donors and the lowest occupied molecular orbital (LUMO) level of acceptors (ΔE_{DA}) and/or work function of metal electrodes [21, 22]. Although the difference between V_{oc} and ΔE_{DA} is still subject to debate, a linear relationship between V_{oc} and ΔE_{DA} has been experimentally confirmed [22]. The HOMO levels of C6TBTAPH₂ and C6PcH₂ were estimated to be 5.25 eV and 5.32 eV, respectively. Hence, the energy gap between the HOMO level of C6TBTAPH₂ and the LUMO level of [70]PCBM tends to be predominant for the V_{oc} of BHJ OSC with the blended donors of C6TBTAPH₂ and C6PcH₂. The fill factors (FF) of the solar cells with various blend ratios of C6PcH₂ were evaluated to be 0.56-0.58.

Table I. J - V characteristics of the C6TBTAPH₂:C6PcH₂:[70]PCBM BHJ OSC with various C6PcH₂ blend ratios.

Blend Ratio of C6PcH ₂ (mol%)	V_{oc} (V)	J_{sc} (mA/cm ²)	FF	PCE (%)
0	0.70	11.3	0.57	4.5
25	0.71	11.6	0.58	4.8
50	0.71	11.3	0.58	4.6
75	0.71	10.9	0.56	4.3
100	0.73	10.6	0.53	4.1

The J_{sc} and PCE of C6TBTAPH₂:C6PcH₂:[70]PCBM BHJ OSC were markedly depending on the C6PcH₂ blend ratio as shown in Fig. 4. The J_{sc} and PCE of C6TBTAPH₂:[70]PCBM BHJ OSC were 11.3 mA/cm² and 4.5%, respectively, while those of C6PcH₂:[70]PCBM BHJ OSC were 10.6 mA/cm² and 4.1%, respectively. In the case of the C6TBTAPH₂:C6PcH₂:[70]PCBM BHJ OSC at 25 mol% of C6PcH₂ blend ratio, the J_{sc} and PCE were improved to be 11.6 mA/cm² and 4.8%, respectively. It is suggested that the enhancement of the J_{sc} mainly contribute to the improvement of the PCE.

Figure 5 shows the EQE spectra of C6TBTAPH₂:C6PcH₂:[70]PCBM BHJ OSC with various C6PcH₂ blend ratios. The main origins of the EQE peaks should be optical excitations at the B-band and Q-band of C6TBTAPH₂ or C6PcH₂. The EQE at B-band in the C6TBTAPH₂:[70]PCBM BHJ OSC is higher than that in the C6PcH₂:[70]PCBM BHJ OSC, while the EQE at Q-band in the C6TBTAPH₂:[70]PCBM BHJ OSC was lower than that in the C6PcH₂:[70]PCBM BHJ OSC. With increasing the blend ratio of C6PcH₂ in the C6TBTAPH₂:C6PcH₂:[70]PCBM BHJ OSC, the EQE at B-band decreased and that at Q-band slightly changed, which must be strongly related with the blend ratio dependence of the absorption spectra as abovementioned.

The EQE is defined as the ratio of the number of charge carriers collected at the electrodes in the solar cell to that of incident photons. In solar radiation spectrum of AM1.5, the number of photons around the wavelength of Q band is about two times more than that at B band. Comparing the EQE spectra at 0 mol% and 25 mol% of C6PcH₂ blend ratios, the quenching of the EQE at B-band with increasing the C6PcH₂ blend ratio seems to be more marked than the enhancement of the EQE at Q-band, however, the enhanced J_{sc} could be confirmed by integrating the EQE spectra indeed. The enhanced J_{sc} could be explained by the photon numbers used for the photon-electron conversion rather

than the EQE. Therefore, the photosensitivity at the Q-band rather than the B-band should be still predominant for the device performance at 0 mol% and 25 mol% of C6PcH₂ blend ratios.

In the case of the C6PcH₂ blend ratio beyond 25 mol%, the absorbance at 400 nm monotonically decreased as shown in Fig. 6. With increasing the C6PcH₂ blend ratio, the absorption loss at B-band should be a main factor, which caused the decreasing of the PCE as well as J_{sc} . As a result, the highest PCE appeared at 25 mol% of C6PcH₂ blend ratio.

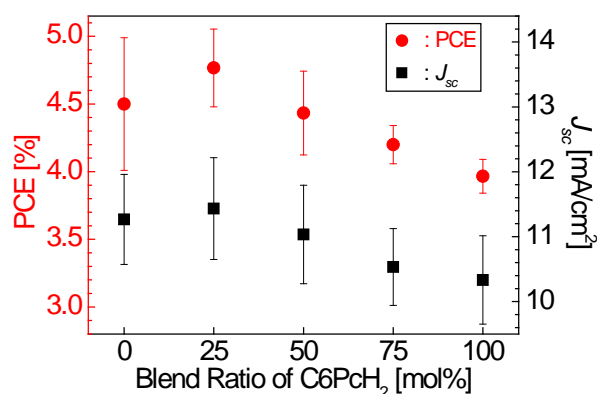


Figure 4. C6PcH₂ blend ratio dependence of the J_{sc} and PCE in the C6TBTAPH₂:C6PcH₂: [70]PCBM BHJ OSC.

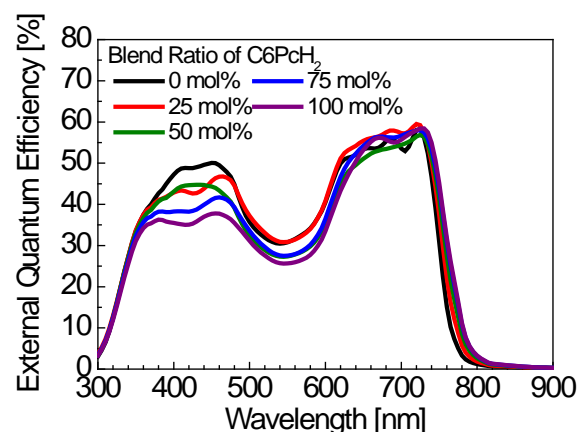


Figure 5. EQE spectra of C6TBTAPH₂:C6PcH₂: [70]PCBM BHJ OSC with various C6PcH₂ blend ratios.

In order to discuss about the carrier transport in the C6TBTAPH₂:C6PcH₂ blended film, the hole mobility as a fundamental property of the blend film was investigated by TOF technique. Figure 6 also shows the C6PcH₂ blend ratio dependence of hole mobility in the blended films of C6TBTAPH₂ and C6PcH₂. The hole mobility in the C6TBTAPH₂ film was 0.23 cm²/Vs. In the blended films below 25 mol% of C6PcH₂ blend ratio, the mobility could not be evaluated, because it is hard to determine the transit time due to the dispersive decay curve with weak photocurrent. The hole mobility could be evaluated to be 0.47 cm²/Vs at 25 mol% of C6PcH₂ blend ratio, and gradually enhanced with increasing the blend ratio of C6PcH₂, eventually 0.96 cm²/Vs at 100 mol% of C6PcH₂. It is noted that the hole mobility changes depending on the blend ratio in spite of the slight difference on the molecular structures and that the blank region of the hole mobility exist below 25 mol% of C6PcH₂ blend ratio.

The crystal structures in the single crystal or thin film were reported to be based on a triclinic lattice for C6TBTAPH₂ and a monoclinic one for C6PcH₂ [23-25]. Further studies exhibited that the crystal structures in blended single crystals of C6TBTAPH₂ and C6PcH₂ at the C6PcH₂ blend ratio below 25 mol% were similar to the triclinic lattice of C6TBTAPH₂ [23]. In the range of 25-100 mol% of C6PcH₂ blend ratio, the crystal structures in the blended single crystals of C6TBTAPH₂ and C6PcH₂ were similar to the monoclinic lattice of C6PcH₂ [23]. It is considered, therefore, that the relatively high hole mobility originated from the C6PcH₂-based molecular packing structure [19].

As shown in Fig. 6, with increasing a blend ratio of C6PcH₂, the hole mobility was enhanced, while the absorbance at B-band was suppressed. At 25 mol% of C6PcH₂ blend ratio, the carrier generation induced by the photo-excitation at Q-band rather than B-band was predominant, and the hole mobility was higher than that of C6TBTAPH₂ because of the C6PcH₂-based crystal structure. Thus, the highest J_{sc} and PCE were achieved at 25 mol% of C6PcH₂ blend ratio.

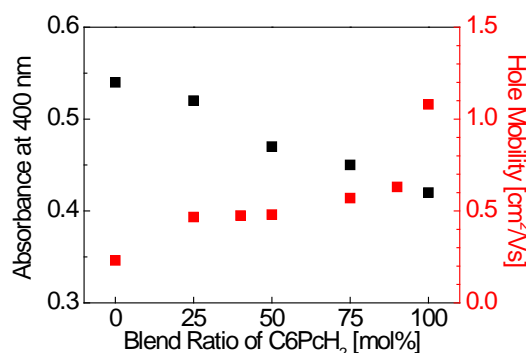


Figure 6. C6PcH₂ blend ratio dependence of the hole mobility in the C6TBTAPH₂:C6PcH₂ blended films and the absorbance at 400 nm of the C6TBTAPH₂:C6PcH₂: [70]PCBM BHJ films.

4. Conclusions

The charge carrier mobility in the blend films of C5PcH₂ and C6PcH₂ were investigated. The phase diagram of the mixture of C5PcH₂ and C6PcH₂ was determined from the thermal properties, it was found that the mixture possess the miscibility. In the case of C5PcH₂ blend ratio below 25 mol%, both hole and electron mobilities were kept high values comparable with those of C6PcH₂, while both hole and electron mobilities markedly decreased by one order of magnitude in the case of C5PcH₂ blend ratio above 30 mol%. From the results of XRD measurement, the molecular structure of the mixture film obviously changed depending on the blend ratio of C5PcH₂, that must be strongly related with the behavior of the charge carrier transport.

Acknowledgements

This work was partly supported by Advanced Low Carbon Technology Research and Development Program from the Japan Science and Technology Agency (JST-ALCA), by JSPS KAKENHI Grant Numbers 15H03552, 26600073, 24246009, and by JSPS Core-to-Core Program, A. Advanced Research Networks.

References

- [1] Schmidt-Mende L, Fechtenkotter A, Mullen K, Moons E, Friend R H and MacKenzie J D 2001 *Science* **293** 1119
- [2] Poll T S, Love J A, Nguyen T Q and Bazan G C 2012 *Adv. Mater.* **24** 3646
- [3] Kyaw A K K, Wang D H, Wynands D, Zhang J, Nguyen T Q, Bazan G C and Heeger A J 2013 *Nano Lett.* **13** 3796
- [4] Walker B, Kim C and Nguyen T Q 2011 *Chem. Mater.* **23** 470
- [5] O'Neil M and Kelly S M 2011 *Adv. Mater.* **23** 566
- [6] Shimizu Y, Oikawa K, Nakayama K and Guilon D 2007 *J. Mater. Chem.* **17** 4223
- [7] Miyake Y, Shiraiwa Y, Okada K, Monobe H, Hori T, Yamasaki N, Yoshida H, Cook M J, Fujii A, Ozaki M and Shimizu Y 2011 *Appl. Phys. Express* **4** 0214604
- [8] Kaafarani B R 2011 *Chem. Mater.* **23** 378
- [9] Sergeyev S, Pisula W and Geerts Y H 2007 *Chem. Soc. Rev.* **36** 1902
- [10] Dao Q D, Hori T, Fukumura K, Masuda T, Kamikado T, Fujii A, Shimizu Y and Ozaki M 2012 *Appl. Phys. Lett.* **101** 263301
- [11] Matsuo Y, Sato Y, Niinomi T, Soga I, Tanaka H and Nakamura E 2009 *J. Am. Chem. Soc.* **131** 16048

- [12] Guide M, Lin J D A, Proctor C M, Chen J, García-Cervera C and Nguyen T Q 2014 *J. Mater. Chem. A* **2** 7890
- [13] Dao Q D, Hori T, Fukumura K, Masuda T, Kamikado T, Fujii A, Shimizu Y and Ozaki M 2013 *Org. Electron.* **14** 2628
- [14] Dao Q D, Watanabe K, Itani H, Sosa-Vargas L, Fujii A, Shimizu Y and Ozaki M 2014 *Chem. Lett.* **43** 1761
- [15] Dao Q D, Sosa-Vargas L, Higashi T, Ohmori M, Itani H, Fujii A, Shimizu Y and Ozaki M 2015 *Org. Electron.* **23** 44
- [16] Fukui H, Nakano S, Uno T, Dao Q D, Saito T, Fujii A, Shimizu Y and Ozaki M 2014 *Org. Electron.* **15** 1189
- [17] Wegewijs B R and Siebbeles L D A 2002 *Phys. Rev. B* **65** 245112
- [18] Schweicher G, Gbabode G, Quist F, Debever O, Dumont N, Sergeyev S and Geerts Y H 2009 *Chem. Mater.* **21** 5867
- [19] Nakagawa D, Nakano C, Ohmori M, Fujii A and Ozaki M 2017 *Org. Electron.* **44** 67
- [20] Fujii A, Itani H, Watanabe K, Dao Q D, Sosa-Vargas L, Shimizu Y and Ozaki M to be published in *Mol. Cryst. & Liq. Cryst.*
- [21] Mihailetchi V D, Blom P W M, Hummelen J C and Rispens M T 2003 *J. Appl. Phys.* **94** 6849
- [22] Yamamoto S, Orimo A, Ohkita H, Bente H and Ito S 2012 *Adv. Energy Mater.* **2** 229
- [23] Nakano C, Ohmori M, Fujii A, Tohnai N and Ozaki M *J. Cryst. Growth* in press
- [24] Ohmori M, Nakano C, Miyano T, Tohnai N, Fujii A and Ozaki M 2016 *J. Cryst. Growth* **445** 9
- [25] Ohmori M, Nakano C, Fujii A, Shimizu Y and Ozaki M *J. Cryst. Growth* in press